JACS
JOURNAL OF THE AMERICAN CHEMICAL SOCIETY

Article

pubs.acs.org/JACS

Assembly and Properties of Heterobimetallic $Co^{II/III}/Ca^{II}$ Complexes with Aquo and Hydroxo Ligands

David C. Lacy,[†] Young Jun Park,[†] Joseph W. Ziller,[†] Junko Yano,[‡] and A. S. Borovik*,[†]

[†]Department of Chemistry, University of California—Irvine, 1102 Natural Sciences II, Irvine, California 92697, United States

[‡]Physical Biosciences Division, Lawrence Berkeley National Laboratory, Berkeley, California 94720, United States

Supporting Information

ABSTRACT: The use of water as a reagent in redox-driven reactions is advantageous because it is abundant and environmentally compatible. The conversion of water to dioxygen in photosynthesis illustrates one example, in which a redox-inactive Ca^{II} ion and four manganese ions are required for function. In this report we describe the stepwise formation of two new heterobimetallic complexes containing $Co^{II/III}$ and Ca^{II} ions and either hydroxo or aquo ligands. The preparation of a four-coordinate Co^{II} synthon was achieved with the tripodal ligand, *N*,*N*′,*N*″-[2,2′,2″-nitrilotris(ethane-2,1-diyl)]-tris(2,4,6-trimethylbenzenesulfonamido, $[MST]^{3-}$. Water binds to $[Co^{II}MST]^-$ to form the five-coordinate $[Co^{II}MST(OH_2)]^-$ complex that was used to prepare the Co^{II}/Ca^{II} complex $[Co^{II}MST(\mu\text{-}OH_2)Ca^{II}\subset 15\text{-crown-}5(OH_2)]^+$ ($[Co^{II}(\mu\text{-}OH_2)\text{-}Ca^{II}OH_2]^+$). $[Co^{II}(\mu\text{-}OH_2)CaOH_2]^+$ contained two aquo ligands, one bonded to the Ca^{II} ion and one bridging between the two metal ions, and thus represents an unusual example of a heterobimetallic complex containing two aquo ligands spanning different metal ions. Both aquo ligands formed intramolecular hydrogen bonds with the $[MST]^{3-}$ ligand. $[Co^{II}MST(OH_2)]^-$ was oxidized to form $[Co^{III}MST(OH_2)]$ that was further converted to $[Co^{III}MST(\mu\text{-}OH)Ca^{II}\subset 15\text{-crown-}5]^+$ ($[Co^{III}(\mu\text{-}OH)Ca^{II}]^+$) in the presence of base and $Ca^{II}OTf_2$/15-crown-5. $[Co^{III}(\mu\text{-}OH)Ca^{II}]^+$ was also synthesized from the oxidation of $[Co^{II}MST]^-$ with iodosylbenzene (PhIO) in the presence of $Ca^{II}OTf_2$/15-crown-5. Allowing $[Co^{III}(\mu\text{-}OH)Ca^{II}]^+$ to react with diphenylhydrazine afforded $[Co^{II}(\mu\text{-}OH_2)Ca^{II}OH_2]^+$ and azobenzene. Additionally, the characterization of $[Co^{III}(\mu\text{-}OH)Ca^{II}]^+$ provides another formulation for the previously reported Co^{IV}–oxo complex, $[(TMG_3tren)Co^{IV}(\mu\text{-}O)Sc^{III}(OTf)_3]^{2+}$ to one that instead could contain a Co^{III}–OH unit.

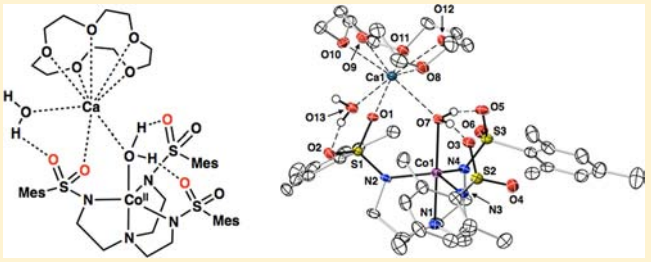

INTRODUCTION

A significant challenge in synthetic chemistry is regulating the secondary coordination sphere of metal ion(s) to affect function.[1] These types of regulatory interactions are found within the active sites of metalloproteins and aid in promoting efficient and selective transformations. Noncovalent interactions are the major forces that control the properties of the secondary coordination spheres in proteins. For instance, intramolecular hydrogen bonds (H-bonds) involving metal-bound water ligands are often found within the structures of active sites and are instrumental in dictating subsequent function. Lipoxygenase is a nonheme iron enzyme that catalyzes the cleavage of C–H bonds by cycling between Fe^{III}–OH and Fe^{II}–OH_2 states.[2] In both states, it is proposed that H-bonding networks involving the hydroxo/aquo ligands are necessary for catalysis. Additionally, recent structural evidence on the oxygen-evolving complex (OEC) within photosystem II has shown that the active site contains an extensive H-bonding network surrounding the terminal aquo ligands on the Mn_4CaO_5 cluster that most likely influences function.[3,4] The OEC also illustrates that calcium ions have an essential role in the oxidation of water to dioxygen.[5] The presence of a Ca^{II} ion within the OEC cluster suggests that group 2 metal ions can influence other redox processes performed by transition-metal complexes. In fact, synthetic molecular water oxidation catalysts often contain a mixture of transition-metal ions and group 1 or 2 ions,[6a] such as in the cobalt/K_3PO_4 system developed by Kanan and Nocera.[6b,c] Recent examples of MnCaO clusters have also been reported; in particular, the Mn_3CaO_4 system of Agapie demonstrated the role of the Ca^{II} ion in modulating redox potentials.[7,8] Nevertheless, the limited number of discrete molecular examples makes it difficult to assess the effects of H-bonds and group 2 metal ions on redox processes at transition-metal ions. Moreover, there are few synthetic examples of heterometallic complexes containing aquo ligands bound similarly to those found in the OEC.

In this report we describe the stepwise assembly of a series of $Co^{II/III}$–OH_2 and Co^{III}–OH complexes from water that contain intramolecular H-bonds and Ca^{II} ions (Chart 1). The complexes are formed using the tripodal ligand *N*,*N*′,*N*″-[2,2′,2″-nitrilotris(ethane-2,1-diyl)]tris-(2,4,6-trimethylbenzenesulfonamido) ($[MST]^{3-}$) that contains three

Received: May 9, 2012
Published: September 22, 2012

   dx.doi.org/10.1021/ja304525n | J. Am. Chem. Soc. 2012, 134, 17526–17535

sulfonamido units. We have shown that this design supports formation of complexes with (Ca^{II}–(μ-OH)–Mn^{III}) cores.[9] The formation of the heterobimetallic Ca/Co complexes in the present study establishes the importance of Ca^{II} ions in stabilizing water binding and is crucial in activating the cobalt center for redox chemistry. Moreover, our findings suggest that the recently reported heterobimetallic complex [(TMG_3tren)-Co^{IV}(μ-O)$Sc^{III}(OTf)_3]^{2+}$, where (TMG_3tren) is tris-(tetramethylguanidino)tren, could be formulated to have a Co^{III}–OH unit rather than the more unusual Co^{IV}–oxo moiety.[10]

Chart 1. Design Aspects of the Heterometallic Complexes

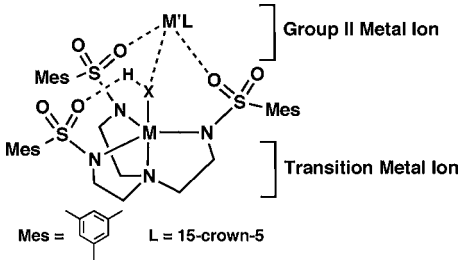

EXPERIMENTAL SECTION

General Methods. All reagents were purchased from commercial sources and used as received, unless otherwise noted. Solvents were sparged with argon and purified using a JC Meyer Co. solvent system. Potassium hydride (KH) as a 30% dispersion in mineral oil was filtered with a medium porosity glass frit and washed five times each with pentane and Et_2O. Solid KH was dried under vacuum and stored under an inert atmosphere. The syntheses of metal complexes were conducted in a Vacuum Atmospheres Co. drybox under an argon atmosphere. The ligand H_3MST,[9] $Ca(OTf)_2$/15-crown-5,[9] [$FeCp_2$]-OTf,[11a] acetyl ferrocenium tetrafluoroborate,[11b] Ca^{II}[N-$(TMS)_2]_2THF_2$,[11c] where $N(TMS)_2$ is bis(trimethylsilyl)amide, and iodosylbenzene (PhIO)[11d] were synthesized according to literature methods. Tetrabutylammonium hexafluorophosphate (TBAP) was recrystallized from hot ethanol three times and dried at 150 °C for several days under reduced pressure.

Preparative Methods. *Preparation of Me_4N[Co^{II}MST].* H_3MST (900 mg, 1.3 mmol) was dissolved in 45 mL of DMA, and KH (160 mg, 3.9 mmol) was added and allowed to stir until gas evolution ceased (~30 min). This solution was allowed to react with $Co^{II}(OAc)_2$ (230 mg, 1.3 mmol) and Me_4N(OAc) (260 mg, 1.9 mmol), and the mixture was allowed to stir overnight. The resulting purple solution was filtered to remove insoluble white material (KOAc, 330 mg, 3.4 mmol, 94% yield), the purple filtrate was concentrated (~5 mL), and Et_2O was added to form a precipitate. The resulting blue solid was isolated on a fritted glass funnel, washed several times with Et_2O, and dried under vacuum for several hours (990 mg, 93%). Further purification of the crude material was possible by dissolving the blue solid in DCM and layering under pentane (660 mg, 62%). Dissolving the crude blue salt in a DMA and MeCN mixture (1:1) and allowing for slow vapor diffusion of Et_2O afforded crystals suitable for X-ray diffraction analysis. FTIR: (KBr, cm^{-1}) selected vibrations 3039, 3021, 2975, 2935, 2874, 2854, 2838, 1655, 1604, 1563, 1488, 1467, 1446, 1405, 1379, 1346, 1279, 1237, 1221, 1141, 1102, 1073, 1055, 1039, 975, 960, 943, 932, 847, 826. UV–vis: λ_{max} [DCM, nm (ε, M^{-1} cm^{-1})] 420 (shoulder), 410 (23), 568 (72), 752 (14). Solid suitable for elemental analysis was recrystallized from DCM/pentane. Anal. calcd (found) for Me_4N[Co^{II}MST]·0.25 DCM ($C_{37.25}H_{57.5}Cl_{0.5}CoN_5O_6S_3$): C, 52.99 (52.68); H, 6.86 (6.91); N, 8.30 (8.33). An alternative method was also utilized: crystalline solid of this salt could be obtained by slow diffusion of Et_2O into the initial DMA filtrate, which after 4 days yielded sky blue crystals (780 mg, 73%).

Preparation of Me_4N[Co^{II}MST(OH_2)]. Me_4N[Co^{II}MST] (99 mg, 0.12 mmol) was dissolved in DCM (~5 mL) and treated with water (20 μL, 1.1 mmol), and the sky blue solution turned pink. Layering the pink solution under pentane produced a crystalline solid of the salt. The pink microcrystals were isolated by decanting and then dried by flowing Ar over the solid for a few seconds (prolonged drying or use of vacuum resulted in loss of the aquo ligand). FTIR: (Nujol, cm^{-1}) ν(OH) 3494, 3186; (KBr, cm^{-1}) ν(OH) 3602, 3497, 3273; selected vibrations (KBr, cm^{-1}) 3022, 2960, 2913, 2856, 1653, 1603, 1563, 1489, 1467, 1451, 1405, 1377, 1384, 1256, 1231, 1133, 1120, 1093, 1055, 1038, 978, 957, 932, 846, 826, 813. UV–vis: λ_{max} [DCM, nm (ε, $M^{-1}cm^{-1}$)] 530 (63), 712 (26). Anal. calcd (found) for Me_4N-[Co^{II}MST(OH_2)]·$2H_2O$ ($C_{37}H_{63}CoN_5O_9S_3$): C, 50.67 (50.73); H, 7.24 (7.18); N, 7.99 (7.79).

Preparation of [Co^{II}MST(μ-OH_2)Ca^{II}⊂15-crown-5-(OH_2)]OTf. Me_4N[Co^{II}MST] (100 mg, 0.12 mmol) was dissolved in 4 mL of DCM, and $Ca^{II}OTf_2$/15-crown-5 (73 mg, 0.13 mmol) was added. After stirring for 5 min, the homogeneous blue solution was treated with water (12 mg, 0.67 mmol), and the solution turned pink. Crystals suitable for diffraction were obtained by layering the pink solution under pentane. Crystallized compound was separated from Me_4NOTf by vigorously stirring with pentane and decanting; the pink salt was isolated on a fritted glass funnel and dried under reduced pressure (111 mg, 63%). FTIR: (Nujol, cm^{-1}) ν(OH) 3430 and 3218; selected vibrations 1604, 1564, 1151, 1124, 1096, 1033, 992, 980, 955, 892, 875, 819. UV–vis: λ_{max} [DCM, nm (ε, $M^{-1}cm^{-1}$)] 530 (49), 698 (28). Anal. calcd (found) for [Co^{II}MST(μ-OH_2)Ca⊂15-crown-5(OH_2)]-OTf·0.5DCM ($C_{44.5}H_{70}CaClCoF_3$ $N_4O_{16}S_4$): C, 43.22 (43.01); H, 5.70 (5.87); N, 4.53 (4.49).

Preparation of [Co^{III}MST(μ-OH)Ca⊂15-crown-5]OTf from H_2O. Me_4N[Co^{II}MST] (100 mg, 0.12 mmol) was suspended in 5 mL of THF, and H_2O (12 mg, 0.67 mmol) was added, causing the mixture to become homogeneous and pink. The solution was then treated with [$FeCp_2$]OTf (40 mg, 0.12 mmol) to produce a dark-red mixture that was stirred for at least 30 min. The mixture was then treated with a 1 mL THF solution containing the following species: Ca^{II}[N-$(TMS)_2]_2(THF)_2$ (45 mg, 0.089 mmol), $Ca^{II}OTf_2$/15-crown-5 (50 mg, 0.090 mmol), and 15-crown-5 (20 mg, 0.091 mmol). This addition resulted in an immediate color change from dark-red to yellow-brown. The solution was stirred for 1 h and filtered, and the THF solvent was removed under reduced pressure. The brown solid was triturated with pentane (3 × 5 mL portions) until the washings were colorless, affording a yellow-brown solid that was dried under reduced pressure. The solid was redissolved in a minimal amount of DCM and stored at −35 °C overnight to produce a white solid (Me_4NOTf) and a small amount of pink crystals ([Co^{II}MST(μ-OH_2)-Ca⊂15-crown-5(OH_2)]OTf) that were removed from the solution via filtration. The resulting yellow-brown filtrate was layered under pentane and stored at −35 °C to produce yellow-brown crystals (44 mg, 31%). Crystals suitable for diffraction were obtained by dissolving the crystalline salt in DCM and layering under pentane at rt. FTIR: (KBr, cm^{-1}) ν(OH) 3430; selected vibrations 3023, 2935, 2858, 1604, 1471, 1405, 1380, 1355, 1265, 1229, 1133, 1090, 1053, 1031, 978, 954, 872, 852, 822. UV–vis: λ_{max} [DCM, nm (ε, $M^{-1}cm^{-1}$)] 390 (4800), 430 (shoulder), 730 (730). ESI-MS(+) calcd (m/z) (found) for [Co^{III}MST(μ-OH)Ca⊂15-crown-5]$^+$ ($C_{43}H_{66}CaCoN_4O_{12}S_3$): 1025.2798 (1025.2771).

Preparation of [Co^{III}MST(μ-OH)Ca⊂15-crown-5]OTf from PhIO. Me_4N[Co^{II}MST] (99 mg, 0.12 mmol) was dissolved in 5 mL of DCM, $Ca^{II}OTf_2$/15-crown-5 (68 mg, 0.12 mmol) was added, and the mixture was stirred until homogeneous. The blue solution was then treated with PhIO (51 mg, 0.23 mmol), causing the blue solution to slowly turn yellow-brown (30 min). Unreacted PhIO was removed by filtration, and the resulting yellow-brown filtrate was concentrated to dryness to afford a solid that was washed with pentane (3 × 10 mL). The solid was extracted with benzene (3 × 10 mL). The benzene solution was reduced to dryness in vacuo. The resulting fine yellow-brown solid was isolated using a fritted glass funnel, washed with pentane, and dried to afford 120 mg (85%) of the desired salt. The

dx.doi.org/10.1021/ja304525n | J. Am. Chem. Soc. 2012, 134, 17526–17535

spectroscopic data match those obtained for samples of the salt made by the previously described method.

Preparation of [Co^{III}MST(OH$_2$)]. $Me_4N[Co^{II}MST]$ (50 mg, 0.061 mmol) was dissolved in 5 mL of DCM and treated with water (5.0 mg, 0.28 mmol), causing a color change from blue to pink. The homogeneous solution was treated with $[FeCp_2]OTf$ (42 mg, 0.13 mmol) resulting in an immediate color change to deep red. After stirring for 30 min, the reaction mixture was filtered, and the DCM filtrate was layered under pentane. A brown-red solid mixture of $[Co^{III}MST(OH_2)]$, unreacted $[FeCp_2]OTf$, and Me_4NOTf was obtained, which was isolated on a fritted glass funnel and washed with pentane until the washings were colorless. The solid was dried (45 mg) and suspended in ~10 mL of toluene, stirred for at least 1 h, and filtered to afford a red filtrate. Pentane (10 mL) was then added to the filtrate, and the mixture was stored at −35 °C, causing the precipitation of pure $[Co^{III}MST(OH_2)]$. The complex was isolated on a fritted glass funnel, washed with pentane, and dried (13 mg, 28%). Crystals suitable for diffraction were obtained by saturating a DCM:pentane solution with pure $[Co^{III}MST(OH_2)]$ and storing at −35 °C for an extended period of time. FTIR: (KBr, cm^{-1}) ν(OH) 3308; selected vibrations 2970, 2936, 2867, 1603, 1564, 1469 1442, 1405, 1388, 1306, 1280, 1144, 1118, 1073, 1051, 1033, 983. UV−vis: λ_{max} [DCM, nm (ε, $M^{-1}cm^{-1}$)] 403 (5700), 494 (5100), 845 (750). Anal. calcd (found) for $[Co^{III}MST(OH_2)]\cdot 0.75$ DCM ($C_{33.75}H_{48.5}Cl_{1.5}CoN_4O_7S_3$): C, 48.80 (49.07); H, 5.89 (6.32); N, 6.75 (6.72).

Physical Methods. Elemental analyses were performed on a Perkin-Elmer 2400 CHNS analyzer. Electronic absorbance spectra were recorded with a Cary 50 and an 8453 Agilent UV−vis spectrophotometer equipped with an Unisoku Unispeks cryostat. Fourier transform infrared spectra were collected on a Varian 800 Scimitar Series FTIR spectrometer. ^{1}H NMR spectra were recorded on a Bruker DRX500 spectrometer. High-resolution mass spectra were collected using Waters Micromass LCT Premier mass spectrometer. Cyclic voltammetric experiments were conducted using a CHI600C electrochemical analyzer. A 2.0 mm glassy carbon electrode was used as the working electrode at scan velocities 0.1 V·s^{-1}. A cobaltocenium/cobaltocene couple (−1.33 V vs $[FeCp_2]^{+/0}$) was used as an internal reference to monitor the reference electrode (Ag^+/Ag). Perpendicular-mode X-band electron paramagnetic resonance (EPR) spectra were collected using a Bruker EMX spectrometer equipped with an ER041XG microwave bridge, an ER4116DM dual-mode cavity, and an Oxford Instrument liquid He quartz cryostat. All EPR spectra were recorded at 10 K with the following experimental parameters: frequency, 9.64 GHz; power, 0.20 mW; modulation amplitude, 9.02 G; time constant, 20.48 s; conversion time, 40.96 s. EPR spectral simulations were done using SpinCount 3.0.[12] Crystals for X-ray diffraction were mounted on a Bruker SMART APEX II diffractometer, and the APEX2 program package was used to determine the unit-cell parameters and for data collection.[12] X-ray absorption spectra were collected at the Stanford Synchrotron Radiation Lightsource (SSRL) on beamlines 7-3 at an electron energy of 3.0 GeV with an average current of 300 mA. The radiation was monochromatized by a Si(220) double-crystal monochromator. The intensity of the incident X-ray (I_0) was monitored by an N_2-filled ion chamber in front of the sample. The data were collected as fluorescence excitation spectra with a Ge 30 element detector (Canberra). Energy was calibrated by the rising edge position of Co foil (7709.0 eV).

RESULTS AND DISCUSSION

Sulfonamido groups have been used by others to prepare multidentate ligands. For instance, the work of Walsh illustrated that C_2 symmetric sulfonamido ligands could be used to synthesize a series of metal complexes.[13] Structural studies on these complexes showed that in some cases both the deprotonated nitrogen donors and the oxygen atoms could bind metal ions to form bridged dinuclear complexes. Sulfonamido groups also have been incorporated into tripodal compounds, but only those ligands of Mountford were used to prepare metal complexes.[14] We have extended the use of sulfonamido-based tripods by preparing $[MST]^{3-}$, which has allowed us to synthesize heterobimetallic complexes.[9] Formation of this type of complex takes advantage of the two structurally distinct metal ion-binding sites on the ligand (Chart 1): One site that is composed of four nitrogen atoms, and a second site that incorporates oxygen atoms of the sulfonamido moieties. The nitrogen-based site can readily bind a transition-metal ion, whereas the oxygen-based site is able to bind main-group metal ions. Furthermore, the sulfonamido groups are positioned to promote the formation of intramolecular H-bonds. We have applied these concepts to assemble a series of Co^{II}−aquo and Co^{III}−OH complexes.

Preparation and Structure of [Co^{II}MST]$^-$. Treating a DMA solution of H_3MST with 3 equiv of KH followed by $Co^{II}(OAc)_2$ and metathesis with $Me_4N(OAc)$ resulted in the formation of $Me_4N[Co^{II}MST]$, which was purified via crystallization. The crystal structure of $Me_4N[Co^{II}MST]$

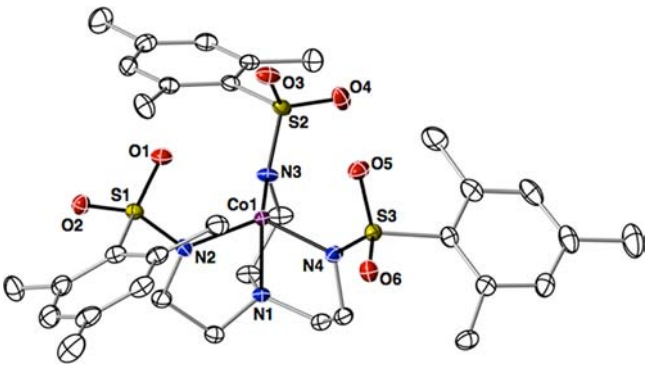

Figure 1. Thermal ellipsoid diagram depicting the molecular structure of $[Co^{II}MST]^-$. The thermal ellipsoids are drawn at the 50% probability level, and the hydrogen atoms are removed for clarity.

revealed that the anion contained a four-coordinate cobalt center having trigonal monopyramidal (TMP) coordination geometry (Figure 1). The average Co−N_{eq} bond length and N_{eq}−Co−N_{eq} angle were 1.967(3) Å and 119.1(2)°, and the Co1−N1 bond distance was 2.114(1) Å (Table 1). The Co^{II}

Table 1. Selected Metrical Data for $[Co^{II}MST]^-$, $[Co^{II}MST(OH_2)]^-$, and $[Co^{III}MST(OH_2)]$

	$[Co^{II}MST]^-$	$[Co^{II}MST(OH_2)]^-$	$[Co^{III}MST(OH_2)]$
	Bond Distances (Å)		
Co1−O7	–	2.135(1)	1.934(2)
Co1−N1	2.114(1)	2.199(1)	1.954(2)
Co1−N2	1.973(1)	2.020(1)	1.950(2)
Co1−N3	1.957(1)	2.028(1)	1.927(2)
Co1−N4	1.971(1)	2.054(1)	1.961(2)
d[Co−N_{eq}][a]	0.207	0.310	0.127
	Bond Angles (°)		
N1−Co1−O7	–	175.52(5)	178.20(7)
N3−Co1−N4	118.90(5)	119.83(5)	119.48(8)
N4−Co1−N2	117.52(5)	119.28(5)	119.43(7)
N3−Co1−N2	120.31(5)	114.04(5)	118.78(7)

[a] d[Co−N_{eq}] is the Co displacement from the equatorial plane formed by three deprotonated sulfonamido nitrogen donors of $[MST]^{3-}$.

dx.doi.org/10.1021/ja304525n | J. Am. Chem. Soc. 2012, 134, 17526−17535

center is displaced 0.207 Å from the plane formed by N2–N4 toward the vacant axial coordination site. These metrical parameters are similar to those of other Co^{II} complexes with TMP geometry.[15a,b,16] The structure of $[Co^{II}MST]^-$ also showed that the SO_2R groups of the $[MST]^{3-}$ ligand formed a cavity around the vacant coordination site on the cobalt center. The UV–vis spectrum of $Me_4N[Co^{II}MST]$ in DCM had absorbance peaks at λ_{max} = 410, 572, and 712 nm (Figure S1); these features are similar to the optical properties found for previously reported TMP Co^{II} complexes.[15a,b,16] Moreover, EPR spectra on frozen DCM solutions of $Me_4N[Co^{II}MST]$ showed that the complex has an $S = 3/2$ spin ground state (Table 2), similar to what is observed in other C_3-symmetric, four-coordinate Co^{II} complexes.[15b,17] Based on these data, we concluded that $[Co^{II}MST]^-$ maintained a TMP structure in solution and could serve as a synthon for the preparation of $Co^{II/III}–OH_2$ and $Co^{III}–OH$ complexes.

Table 2. EPR and Redox Properties of the Co^{II} Complexes

complex	*g*-values	A_z (cm^{-1})	$E_{1/2}$ (V)[a]
$[Co^{II}MST]^-$	4.36, 2.00	96×10^{-4}	0.41
$[Co^{II}MST]^- + Ca^{II}$	4.31, 2.00	94×10^{-4}	0.62
$[Co^{II}MST(OH_2)]^-$	4.33, 2.04	90×10^{-4}	0.068
$[Co^{II}(\mu\text{-}OH_2)Ca^{II}OH_2]^+$	4.35, 2.02	98×10^{-4}	0.29

[a]Versus $[FeCp_2]^{+/0}$.

Preparation and Structures of Co^{II}–Aquo Complexes. The synthesis of $[Co^{II}MST]^-$ allowed us to examine the stepwise binding of external species to the complex. This process is illustrated with the preparation of the monoaquo Co^{II} complex $[Co^{II}MST(OH_2)]^-$, which was accomplished by treating a DCM solution of $[Co^{II}MST]^-$ with excess H_2O causing a color change from sky blue to pink (Scheme 1). The UV–vis spectrum of $[Co^{II}MST(OH_2)]^-$ is similar to that found for the $Co^{II}–OH$ complex $[Co^{II}H_3buea(OH)]^{2-}$ (where $[H_3buea]^{3-}$ is tris(*tert*-butylureaylethylene)aminato), which has a trigonal bipyramidal (TBP) coordination geometry.[15c] The molecular structure of the complex was determined by X-ray diffraction methods and confirmed the trigonal bipyramidal coordination geometry of the cobalt center (Figure 2). The binding of the water molecule occurs at the open site within the sulfonamido cavity, having a Co1–O7 bond distance of 2.135(1) Å and an O7–Co1–N1 bond angle of 175.52(5)°. Minor structural differences in bond lengths of less than 0.085 Å were found between $[Co^{II}MST]^-$ and $[Co^{II}MST(OH_2)]^-$. In addition, the Co^{II} ion is displaced 0.310 Å from the plane formed by N2–N4 atoms of $[MST]^{3-}$, a change of greater than 0.1 Å from that observed in $[Co^{II}MST]^-$. The aquo ligand also forms two intramolecular H-bonds to the O3 and O5 atoms of $[MST]^{3-}$ as indicated by the O7···O3 and O7···O5 distances of 2.677(2) Å.

The binding of water to $[Co^{II}MST]^-$ also occurred when Ca^{II} ions were added to the complex. In the presence of $CaOTf_2$/15-crown-5 and 5 equiv H_2O (Scheme 1), a new species was isolated whose analytical and vibrational properties suggested the formation of a heterobimetallic complex containing a $Co^{II}–(\mu\text{-}OH_2)–Ca^{II}$ core. The visible spectrum of this species measured in DCM was similar to $[Co^{II}MST(OH_2)]^-$, a finding that is consistent with the complex maintaining a Co^{II}–aquo unit with trigonal bipyramidal coordination geometry (Figure S1).[18]

Determination of the molecular structure of this new species revealed the heterobimetallic complex $[Co^{II}MST(\mu\text{-}OH_2)$-

Scheme 1. Preparative Routes to the Cobalt Complexes[a]

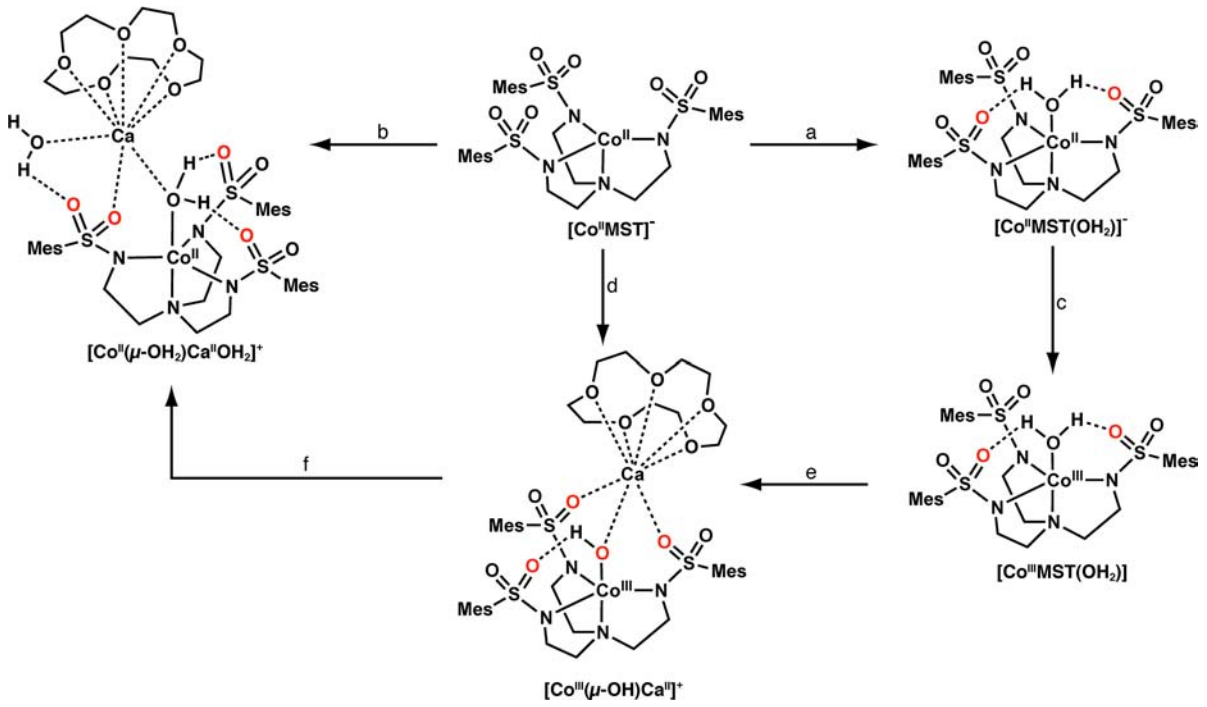

[a]Conditions: (a) 5–10 equiv H_2O, rt, DCM; (b) $Ca(OTf)_2$/15-crown-5, 5 equiv H_2O, rt, DCM; (c) $[Fe^{III}Cp_2]OTf$, rt, DCM (or THF); (d) $Ca(OTf)_2$/15-crown-5, PhIO, rt, DCM; (e) 0.5 equiv $Ca[N(TMS)_2]_2{\cdot}THF_2$, 0.5 equiv 15-crown-5, and equiv 0.5 $Ca(OTf)_2$/15-crown-5, rt, THF; (f) 10 equiv DPH, rt, DCM.

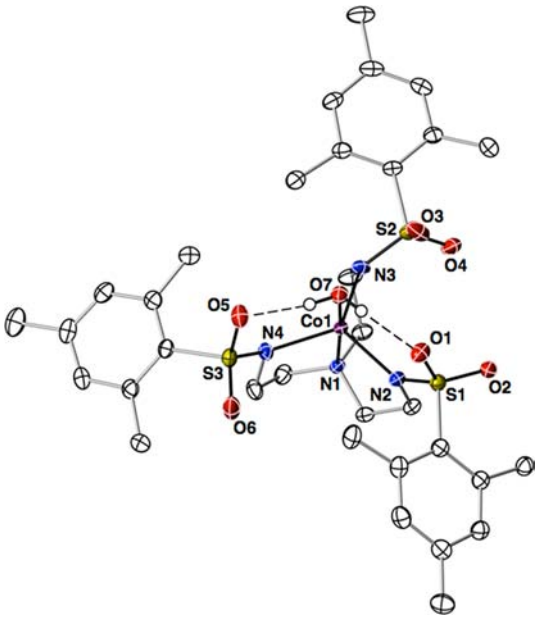

Figure 2. Thermal ellipsoid diagram depicting the molecular structure of $[Co^{II}MST(OH_2)]^-$. The thermal ellipsoids are drawn at the 50% probability level, and only the hydrogen atoms of the water ligand are shown for clarity.

$Ca^{II}\subset$15-crown-5$(OH_2)]^+$ ($[Co^{II}(\mu\text{-}OH_2)Ca^{II}OH_2]^+$) (Figure 3). As in $[Co^{II}MST(OH_2)]^-$, the Co^{II} ion accommodates a single aquo ligand; however, the aquo ligand bridges the Co^{II} and Ca^{II} ions to form the $Co^{II}-(\mu\text{-}OH_2)-Ca^{II}$ core. There are several small changes in the metrical parameters around the Co^{II} ion as compared to those in $[Co^{II}MST(OH_2)]^-$. For

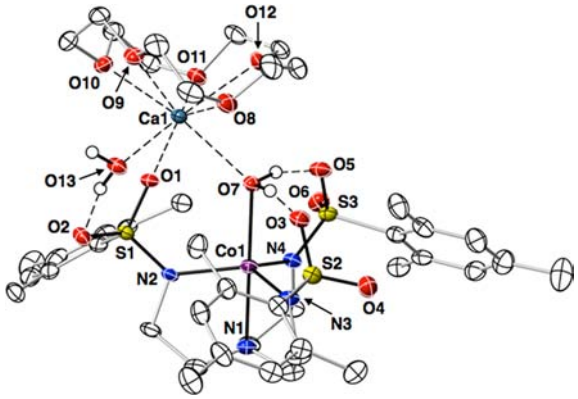

Figure 3. Thermal ellipsoid diagram depicting the molecular structure of $[Co^{II}(\mu\text{-}OH_2)Ca^{II}OH_2]^+$. The thermal ellipsoids are drawn at the 50% probability level, and only the hydrogen atoms of the water ligands are shown for clarity.

instance, the Co1−O7 bond length of 2.221(2) Å in $[Co^{II}(\mu\text{-}OH_2)Ca^{II}OH_2]^+$ is elongated by 0.086 Å. In addition, the Co^{II} ion in $[Co^{II}(\mu\text{-}OH_2)Ca^{II}OH_2]^+$ is slightly more displaced out of the trigonal plane by 0.015 Å. The bridging aquo ligand also forms two intramolecular H-bonds as indicated by the O7···O3 and O7···O5 distances of 2.656(2) and 2.693(2) Å. These changes suggested that the Ca^{II} ion does not perturb the primary coordination sphere of the Co^{II} ion to a large extent, in agreement with the optical spectrum.

In addition to the small changes in the primary coordination sphere of the Co^{II} center, there are several new structural features within the secondary coordination sphere. The $[Co^{II}MST(OH_2)]^-$ moiety acts as a bidentate ligand to the Ca^{II} ion through the bridging aquo O7 atom and the O1 atom from a sulfonamido group with a Ca1−O1 bond distance of 2.399(1) Å and a longer Ca1−O7 length of 2.531(2) Å. The structure of $[Co^{II}(\mu\text{-}OH_2)Ca^{II}OH_2]^+$ also showed that the complex had a second terminal aquo ligand bonded to the Ca^{II} ion. The Ca1−O13 bond length of 2.369(2) Å is significantly shorter than the distance observed for the Ca1−O7 bond by 0.16 Å. The terminal aquo also forms a single intramolecular H-bond with an O13···O2 distance of 2.758(2) Å. The oxygen atoms of the 15-crown-5 ligand fill the remaining coordination sites on the Ca^{II} ion. The structure of $[Co^{II}(\mu\text{-}OH_2)Ca^{II}OH_2]^+$ also showed that the two aquo ligands are relatively close to one another, having an O7···O13 interatomic distance of 3.762(3) Å.

Even though the structural properties of the primary coordination sphere of the Co^{II} center in $[Co^{II}MST(OH_2)]^-$ and $[Co^{II}(\mu\text{-}OH_2)Ca^{II}OH_2]^+$ are nearly the same, the addition of Ca^{II} ion affects the lability of Co−OH_2 unit in the solid state. Conversion of $[Co^{II}MST(OH_2)]^-$ to $[Co^{II}MST]^-$ was accomplished by simply applying a small vacuum ($P \sim 10^{-3}$ Torr). However, attempts to remove either the terminal or bridging aquo ligands in $[Co^{II}(\mu\text{-}OH_2)Ca^{II}OH_2]^+$ were unsuccessful, even after prolonged exposure to vacuum, determined by comparison of FTIR spectra (Figure S2B) and elemental analyses to those obtained from independently prepared samples of $[Co^{II}(\mu\text{-}OH_2)\text{-}Ca^{2+}\subset$15-crown-5-$(OH_2)]OTf$.

Electrochemical and EPR Properties. The redox properties of the Co^{II} complexes were explored using cyclic voltammetry in DCM (Figures 4A and S3, Table 2). For

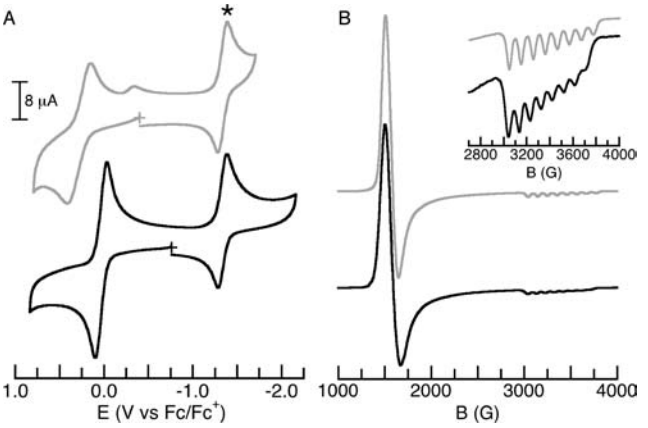

Figure 4. Cyclic voltammograms (A) and ⊥-mode EPR spectra (B) of $[Co^{II}MST(OH_2)]^-$ (black line) and $[Co^{II}(\mu\text{-}OH_2)Ca^{II}OH_2]^+$ (gray line). Cobaltocenium (*) was used as an internal standard in the CV experiments. The voltammograms were recorded at rt in DCM (with 0.1 M $TBAPF_6$), and the EPR data were collected at 10 K on frozen DCM solution (6 mM). Inset: comparison of the hyperfine interactions for the two Co^{II}−aquo complexes. See Table 2 for $E_{1/2}$ and g- and A_z-values.

$[Co^{II}MST]^-$, a reversible one-electron process was observed at 0.41 V vs $[FeCp_2]^{+/0}$ that is assigned to the $Co^{II/III}$ couple. The potential shifted to more positive values when Ca^{II} ions were introduced to the electrochemical cell. Treating $[Co^{II}MST]^-$ with 1 equiv $Ca(OTf)_2$/15-crown-5 produced a new quasi-reversible couple at 0.62 V vs $[FeCp_2]^{+/0}$, suggesting that Ca^{II}

dx.doi.org/10.1021/ja304525n | J. Am. Chem. Soc. 2012, 134, 17526−17535

ions can interact with $[Co^{II}MST]^-$ in the absence of an external ligand within the cavity (Figure S3).

The electrochemical properties of the $Co^{II}-OH_2$ complexes were substantially different from $[Co^{II}MST]^-$. For $[Co^{II}MST(OH_2)]^-$, a reversible couple was found at 0.068 V, a shift of nearly 0.4 V from that of $[Co^{II}MST]^-$. This shift is consistent with a more facile oxidation of a five-coordinate Co^{II} center than one that is four-coordinate. The $Co^{II/III}$ potential for $[Co^{II}(\mu\text{-}OH_2)Ca^{II}OH_2]^+$ appeared at 0.29 V vs $[FeCp_2]^{+/0}$, a shift of more than 0.2 V compared to $[Co^{II}MST(OH_2)]^-$. The increase in redox potential reflects that change in overall positive charge of the complex upon the binding of the Ca^{II} ion.

The ⊥-mode EPR spectra measured on frozen solutions of the Co^{II} complexes all have features with g-values centered near 4.3 and 2.0, which is indicative of $S = 3/2$ spin ground states.[17] However, there are distinguishable differences in the g-values (Figures 4B and S4, Table 2) that reflect the changes in the coordination environments of the complexes. In addition, the complexes have similar eight-line hyperfine patterns on the features at $g \sim 2.0$ (Table 2), which is consistent with monomeric Co^{II} species. Notice that the largest difference in the hyperfine splitting ($\Delta A_z = 8 \times 10^{-4}$ cm^{-1}) is observed between the two $Co^{II}-OH_2$ species, $[Co^{II}MST(OH_2)]^-$ and $[Co^{II}(\mu\text{-}OH_2)Ca^{II}OH_2]^+$.

Synthesis and Structure of $[Co^{III}MST(OH_2)]$. The reversible $Co^{II/III}$ couple measured for $[Co^{II}MST(OH_2)]^-$ prompted our investigation into isolating this oxidized product by chemical methods. We found that treating $[Co^{II}MST(OH_2)]^-$ with $[Fe^{III}Cp_2]OTf$ in DCM (or THF) resulted in an immediate color change from pink to deep red (Scheme 1, Figure S5). The optical spectrum in DCM of the new species revealed intense features at λ_{max} (ε_M) = 403 (5700), 494 (5100), 845 (750) nm that are characteristic of Co^{III} complexes with TBP geometry.[15c] Additional spectroscopic and analytical measurements suggested that this new red species was the expected $Co^{III}-OH_2$ complex, $[Co^{III}MST(OH_2)]$. We also investigated this oxidative process in the presence of $Ca(OTf)_2$/15-crown-5 and found that the reaction was incomplete when using $[Fe^{III}Cp_2]OTf$ as the oxidant, which agrees with our electrochemical observations. Complete conversion to an oxidized species was accomplished using the stronger oxidant acetyl ferrocenium tetrafluoroborate ($E_{1/2}$ = 0.27 V vs $[FeCp_2]^{+/0}$);[11b] this complex had optical properties nearly identical to those of $[Co^{III}MST(OH_2)]$, but we were unable to obtain the complex in sufficient purity to determine its formulation.

The molecular structure of $[Co^{III}MST(OH_2)]$ showed that the primary coordination sphere of the cobalt center had the expected contraction compared to its $Co^{II}-OH_2$ analog (Table 1 and Figure S6). The Co1–N1 bond distance in $[Co^{III}MST(OH_2)]$ is 1.954(2) Å, and its average Co1–N_{eq} bond distance is 1.946 Å, which are shorter by 0.245 and 0.088 Å, respectively, compared to those in $[Co^{II}MST(OH_2)]^-$. In addition, the Co1–O7 bond distance in $[Co^{III}MST(OH_2)]$ decreased by 0.201 Å upon oxidation to 1.934(2) Å. There are also intramolecular H-bonds between the aquo ligand and $[MST]^{3-}$ in $[Co^{III}MST(OH_2)]$, yet the O7···O1 and O7···O5 distances of 2.589 and 2.576 Å are significantly shorter than those found in $[Co^{II}MST(OH_2)]^-$. The shortening of these distances corresponds to a strengthening of the H-bonds in $[Co^{III}MST(OH_2)]$, which is expected because the acidity of the aquo ligand will increase upon coordination to the Co^{III} center. This premise is further supported by FTIR studies: The ν(O–H) bands in $[Co^{III}MST(OH_2)]$ are broadened and at lower energies than those found in $[Co^{II}MST(OH_2)]^-$.

Oxidation Chemistry: Preparation and Structure of $[Co^{III}MST(\mu\text{-}OH)\text{-}Ca\subset 15\text{-}crown\text{-}5]^+$. $[Co^{II}MST]^-$ did not react with dioxygen even in the presence of Ca^{II} ions, in agreement with our electrochemical measurements. The reactivity of $[Co^{II}MST]^-$ with PhIO was also explored, and we found no evidence for a reaction, even after several days. However, when $[Co^{II}MST]^-$ was treated with PhIO in the presence of $Ca(OTf)_2$/15-crown-5, a new dark-yellow-brown species was formed within 1 h (Scheme 1). The new species had an absorption spectrum in DCM with features at λ_{max} (ε_M) = 390 (4800), 430 (sh), 730 (730) nm, which are similar to another monomeric TBP $Co^{III}-OH$ complex (Figure S5).[15c] Electrospray ionization high-resolution mass spectrometry (ESI-HRMS) results showed a species with a strong ion peak with mass-to-charge ratio (m/z) of 1025.2771 (calcd, 1025.2798), corresponding to a species having a formulation of $[Co^{III}MST(\mu\text{-}OH)\text{-}Ca\subset 15\text{-}crown\text{-}5]^+$ ($[Co^{III}(\mu\text{-}OH)Ca^{II}]^+$). Furthermore, FTIR analysis revealed a sharp peak at 3430 cm^{-1} supporting the presence of a hydroxo ligand (Figure S7).

Repeated attempts to crystallize $[Co^{III}(\mu\text{-}OH)Ca^{II}]^+$ synthesized from PhIO were unsuccessful, and thus a new synthetic route was sought. We reasoned that deprotonation of $[Co^{III}MST(OH_2)]$ with an appropriate base could lead to a putative $Co^{III}-OH$ complex which could then be treated with $Ca(OTf)_2$/15-crown-5 to form $[Co^{III}(\mu\text{-}OH)Ca^{II}]^+$. This approach was realized by treating a THF solution of $[Co^{III}MST(OH_2)]$ with 0.5 equiv $Ca[N(TMS)_2]_2{\cdot}THF_2$, 0.5 equiv 15-crown-5, and 0.5 equiv $Ca(OTf)_2$/15-crown-5 that produced a species that had identical spectroscopic properties to $[Co^{III}(\mu\text{-}OH)Ca^{II}]^+$ (Scheme 1). Moreover, this approach yielded single crystals that were suitable for X-ray structural determination, thereby confirming the mass spectral formulation of the yellow-brown species as $[Co^{III}MST(\mu\text{-}OH)\text{-}Ca\subset 15\text{-}crown\text{-}5]^+$ (Figure 5). The molecular structure of $[Co^{III}(\mu\text{-}OH)Ca^{II}]^+$ contained a hydroxo ligand bridging the Co^{III} center and the Ca^{II} ion, in a manner similar to the manganese analog.[9] The Co^{III} center has TBP coordination geometry provided by the nitrogen donors of the $[MST]^{3-}$ and the hydroxo ligands. The Co1–N1 and Co1–N_{eq} bond distances are comparable to those found for $[Co^{III}MST(OH_2)]$. However, the Co1–O7

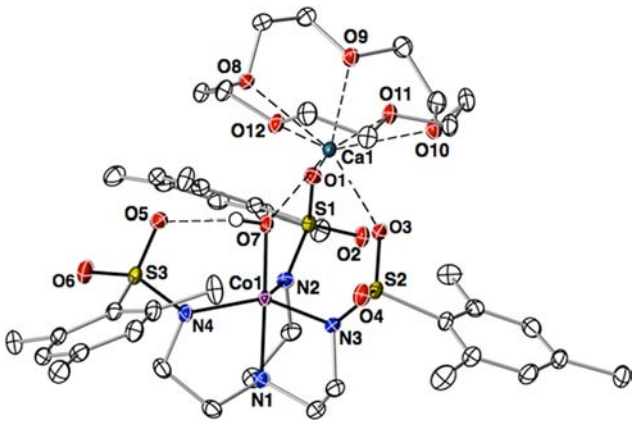

Figure 5. Thermal ellipsoid diagram depicting the molecular structure of $[Co^{III}(\mu\text{-}OH)Ca^{II}]^+$. The thermal ellipsoids are drawn at the 50% probability level, and only the hydrogen atom of the hydroxo ligand is shown for clarity.

dx.doi.org/10.1021/ja304525n | J. Am. Chem. Soc. 2012, 134, 17526–17535

bond distance in $[Co^{III}(\mu\text{-}OH)Ca^{II}]^+$ is 1.854(1) Å,[19] a decrease in length of 0.080 Å from $[Co^{III}MST(OH_2)]$ and 0.367 Å from $[Co^{II}(\mu\text{-}OH_2)Ca^{II}OH_2]^+$. The N1−Co1−O7 bond angle in $[Co^{III}(\mu\text{-}OH)Ca^{II}]^+$ is statistically equivalent to that in $[Co^{II}(\mu\text{-}OH_2)Ca^{II}OH_2]^+$, whereas the Ca1−O7 bond distance in $[Co^{III}(\mu\text{-}OH)Ca^{II}]^+$ is 0.265 Å shorter than that in $[Co^{II}(\mu\text{-}OH_2)Ca^{II}OH_2]^+$. In addition, there is a large contraction of the Co1−Ca1 interatomic distance of over 0.5 Å between $[Co^{II}(\mu\text{-}OH_2)Ca^{II}OH_2]^+$ and $[Co^{III}(\mu\text{-}OH)Ca^{II}]^+$.

A comparison of the molecular structures of $[Co^{II}(\mu\text{-}OH_2)Ca^{II}OH_2]^+$ and $[Co^{III}(\mu\text{-}OH)Ca^{II}]^+$ (Table 3) illustrates

Table 3. Comparison of Metrical Parameters for $[Co^{III}(\mu\text{-}OH)Ca^{II}]^+$ and $[Co^{II}(\mu\text{-}OH_2)Ca^{II}OH_2]^+$

	$[Co^{III}(\mu\text{-}OH)\text{-}Ca^{II}]^+$	$[Co^{II}(\mu\text{-}OH_2)\text{-}Ca^{II}OH_2]^+$
	Bond Distances (Å)	
Co1−O7	1.854(1)	2.221(2)
Co1−N1	1.997(1)	2.126(2)
Co1−N2	1.971(2)	2.037(2)
Co1−N3	1.950(2)	2.031(2)
Co1−N4	1.962(2)	2.013(2)
Ca1−O1	2.361(2)	2.399(1)
Ca1−O3	2.379(1)	–
Ca1−O7	2.266(1)	2.531(2)
Ca1−O13	–	2.369(2)
Ca1···Co1	3.804(1)	4.315(1)
$d[Co-N_{eq}]^a$	0.212	0.325
	Bond Angles (°)	
N1−Co1−O7	177.38(6)	177.75(7)
Co1−O7−Ca1	134.56(7)	130.41(7)
O7−Ca1−O13	–	100.29(6)
N3−Co1−N4	124.35(7)	113.87(8)
N4−Co1−N2	123.14(7)	114.14(8)
N3−Co1−N2	109.01(7)	124.40(8)

[a] $d[Co-N_{eq}]$ is the Co displacement from the equatorial plane formed by three deprotonated sulfonamido nitrogen donors of $[MST]^{3-}$.

the versatility of the $[MST]^{3-}$ ligand to accommodate a second metal ion and form intramolecular H-bonds. In $[Co^{III}(\mu\text{-}OH)Ca^{II}]^+$ a single intramolecular H-bond between the hydroxo ligand and O5 of the $[MST]^{3-}$ ligand was present. Because of this lone H-bond, the remaining sulfonamido groups, along with the hydroxo ligand, formed a tridentate-binding site for the calcium ion; binding to the Ca^{II} ion occurred through O7 and the O1 and O3 atoms of the sulfonamido groups. In $[Co^{II}(\mu\text{-}OH_2)Ca^{II}OH_2]^+$, the bridging aquo ligand (the one containing O7) is involved in two intramolecular H-bonds with the $[MST]^{3-}$ ligand. Thus, the O1 atom of the remaining sulfonamido group and O7 act as a bidentate ligand to the calcium center. These results suggest that $[MST]^{3-}$ can regulate the mode of coordination to a second metal ion depending on the type of intramolecular H-bonding network in the complex.

The reactivity of $[Co^{III}(\mu\text{-}OH)Ca^{II}]^+$ with diphenylhydrazine (DPH) was also explored. $[Co^{III}(\mu\text{-}OH)Ca^{II}]^+$ reacts slowly with 0.5 equiv of DPH at rt. However, when 10 equiv of DPH were employed, $[Co^{III}(\mu\text{-}OH)Ca^{II}]^+$ was converted to a new species in less than 20 min, whose EPR spectrum was identical to that of $[Co^{II}(\mu\text{-}OH_2)Ca^{II}OH_2]^+$ (Figures S8 and S9), along with the formation of azobenzene in a yield of 70%.

Comparison of $[Co^{III}(\mu\text{-}OH)Ca^{II}]^+$ to a Proposed $[Co^{IV}(\mu\text{-}O)Sc^{III}]^{2+}$ Complex. We compared the properties of the $Co^{III/II}$ complexes with $[MST]^{3-}$ to other cobalt complexes with C_3 symmetric ligands.[10,15] In particular, we found noticeable similarities in the reactivity and physical properties to complexes synthesized by Ray derived from $[Co^{II}TMG_3tren(OTf)]^+$, a five-coordinate Co^{II} complex with a tripodal ligand that is comparable to $[MST]^{3-}$.[10] Both $[Co^{II}MST]^-$ and $[Co^{II}TMG_3tren(OTf)]^+$ are only oxidized with oxygen-atom transfer reagents in the presence of redox-inactive metal ions. Ray reported that treating $[Co^{II}TMG_3tren(OTf)]^+$ with 2-(*tert*-butylsulfonyl)iodosylbenzene (^{s}PhIO) and $Sc(OTf)_3$ produced a new species formulated as $[(TMG_3tren)Co^{IV}(\mu\text{-}O)\text{-}Sc^{III}(OTf)_3]^{2+}$ (Scheme 2A), whose EPR features were assigned

Scheme 2. Comparison of Possible Heterobimetallic Complex Formed When Treating $[Co^{II}TMGtren(OTf)]^+$ with ^{s}PhIO and $Sc(OTf)_3$ as Proposed in the Literature[10] (A) and Reformulated Based on the Results Obtained Herein (B)

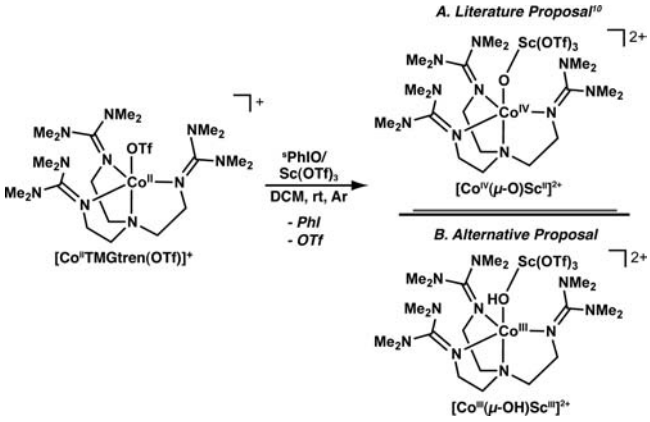

to a $Co^{IV}(\mu\text{-}O)Sc^{III}$ core having a $S = 3/2$ spin ground state. This presumed Co^{IV} product had a visible spectrum with features at λ_{max} = 489 and 810 nm that are strikingly similar to those found for $[Co^{III}(\mu\text{-}OH)Ca^{II}]^+$ (Figure S5) and other Co^{III}−O(H) species.[15c,d] Using EXAFS methods, a Co−O bond length of 1.85 Å was found in $[(TMG_3tren)Co^{IV}(\mu\text{-}O)Sc^{III}(OTf)_3]^{2+}$, which was used as evidence for a Co^{IV}−oxo unit; yet this bond length is identical to the Co1−O7 bond distance of 1.854(2) Å found by X-ray diffraction methods for $[Co^{III}(\mu\text{-}OH)Ca^{II}]^+$.[19] Moreover, data from X-ray absorption near-edge spectra (XANES) showed a 1.25 eV shift in edge energies between $[Co^{II}TMG_3tren]^{2+}$ and the $[(TMG_3tren)\text{-}Co^{IV}(\mu\text{-}O)Sc^{III}(OTf)_3]^{2+}$ complex. The XANES spectra for both $[Co^{II}(\mu\text{-}OH_2)Ca^{II}OH_2]^+$ and $[Co^{III}(\mu\text{-}OH)Ca^{II}]^+$ have also been measured[20] (Figure 6), and we found an edge energy shift of 1.42 eV even though the cobalt centers in our complexes differ by only one oxidation state. From these results we propose that treating $[Co^{II}TMG_3tren(OTf)]^+$ with ^{s}PhIO in the presence of Sc^{3+} ions produced a metastable $[(TMG_3tren)\text{-}Co^{III}(\mu\text{-}OH)Sc^{III}(OTf)_3]^{2+}$ complex rather than the Co^{IV}−oxo analog proposed previously (Scheme 2B). Our premise is supported by the similarities in the electronic and structural properties of the oxidized product of $[Co^{II}TMG_3tren(OTf)]^+$ with those found in other Co^{III}−hydroxo complexes, including $[Co^{III}(\mu\text{-}OH)Ca^{II}]^+$. A $[(TMG_3tren)Co^{III}(\mu\text{-}OH)\text{-}Sc^{III}(OTf)_3]^{2+}$ complex should also have analogous types of reactivity as we observed for $[Co^{III}(\mu\text{-}OH)Ca^{II}]^+$; namely it can

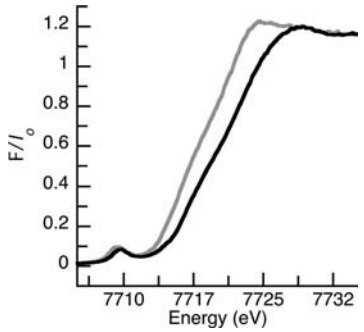

Figure 6. XANES spectra for $[Co^{II}(\mu\text{-}OH_2)Ca^{II}OH_2]^+$ (gray line) and $[Co^{III}(\mu\text{-}OH)Ca^{II}]^+$ (black line) collected on solid samples (10% by weight) in boron nitride.[20]

react with X−H bonds to produce a Co^{II}-containing species. Our proposal suggests that both Co^{III} and Co^{II} complexes could be present at the same time[21] and accounts for the observation of a $S = 3/2$ species (i.e., these EPR features are derived from a Co^{II} center, rather than Co^{IV}). Note that the EPR parameters, specifically the hyperfine interactions, between the putative Ray's Co^{IV}−oxo complex and our $[Co^{II}(\mu\text{-}OH_2)Ca^{II}OH_2]^+$ are nearly identical (A_z = 100 × 10^{-4} and 98 × 10^{-4} cm^{-1}, respectively).

SUMMARY

We have demonstrated for the first time the stepwise generation of Co−aquo complexes that led to the isolation of a system containing a $Co^{II}(\mu\text{-}OH_2)Ca^{II}OH_2$ core, a motif resembling structural elements found in the OEC. The active site includes both transition-metal ions (Mn) and a Ca^{II} ion, in addition to an extensive H-bonding network, and all these features are critical for water oxidation.[3,4] The presence of a Ca^{II} ion in the OEC has prompted several synthetic efforts to prepare transition-metal clusters that include calcium ions.[5−9] In addition, intramolecular H-bonds have been proposed to be involved in some synthetic water oxidation systems[22] and have been used to isolate metal−aquo complexes.[23] However, incorporation of a Ca^{II} ion, transition-metal ions, at least two water molecules, and an intramolecular H-bond network into a single molecular species has been difficult to replicate in synthetic systems. We accomplished the synthesis of this type of heterobimetallic complex using the multifunctional tripodal ligand $[MST]^{3-}$, which coordinated both Ca^{II} and Co^{II} ions, as it positioned two aquo ligands within 3 Å of each other. Its design took advantage of noncovalent interactions that linked the two metal centers and stabilized the aquo ligands through intramolecular H-bonds. Utilizing noncovalent interactions produced versatile systems in which the cobalt and Ca^{II} centers could readily adopt different primary and secondary coordination spheres.

Changes in redox properties of the Co^{II} complexes correlated with the coordination of Ca^{II} ions. For example, the redox potential of the $[Co^{II}MST]^-$ shifted over 200 mV in the presence of Ca^{II} ions. A similar positive shift was observed when Ca^{II} ions were added to $[Co^{II}MST(OH_2)]^-$. Moreover, $[Co^{II}MST]^-$ does not react with dioxygen but only with stronger oxidants, such as PhIO, in the presence of Ca^{II} ions to afford the heterobimetallic complex $[Co^{III}(\mu\text{-}OH)Ca^{II}]^+$. The dependency of this reaction on Ca^{II} ions suggests an inner sphere process, whereby the Ca^{II} ion is essential for binding and oxidation. The need for Ca^{II} ions to promote reactivity is similar to what we observed in the synthesis of the analogous $[Mn^{III}(\mu\text{-}OH)Ca^{II}]^+$ species.[9,24]

The conversion of $[Co^{III}(\mu\text{-}OH)Ca^{II}]^+$ to $[Co^{II}(\mu\text{-}OH_2)\text{-}Ca^{II}OH_2]^+$ when treated with DPH illustrated that Co^{III}−OH complexes can homolytically cleave X−H bonds. This type of reactivity is observed in the enzyme lipoxygenase which utilizes $Fe^{III}OH$ species to cleave C−H bonds.[2] Similar X−H bond cleavage reactivity by synthetic M^{III}−OH complexes is known,[25] but to our knowledge $[Co^{III}(\mu\text{-}OH)Ca^{II}]^+$ is the first example of a Co^{III}−OH species exhibiting this kind of chemistry. This finding, along with the structural and physical properties of $[Co^{III}(\mu\text{-}OH)Ca^{II}]^+$ and $[Co^{II}(\mu\text{-}OH_2)Ca^{II}OH_2]^+$, indicated that the recently reported Co^{IV}−oxo species[10] is likely a complex containing a Co^{III} center. Theoretical studies using DFT methods on in silico generated Co^{IV}−oxo species suggest that the oxo ligand can have appreciable spin density,[10,26] leading to the possibility of Co^{III}−oxyl radical complexes. We think it is an unlikely assignment based on the experimental data presented here, which is consistent with the more plausible formulation of a $Co^{III}(\mu\text{-}OH)Sc^{III}$ core.

ASSOCIATED CONTENT

Supporting Information

Crystallographic details for all the molecular structures with CIFs and Figures S1−S9. This material is available free of charge via the Internet at http://pubs.acs.org.

AUTHOR INFORMATION

Corresponding Author

aborovik@uci.edu

Notes

The authors declare no competing financial interest.

ACKNOWLEDGMENTS

We thank the NIH (GM50781) for support of this work. Portions of this research were supported by the Department of Energy (DOE), Office of Science, Office of Basic Energy Science (OBES), Division of Chemical Sciences, Geosciences, and Biosciences, under contract DE-AC02-05CH11231, and carried out at the Stanford Synchrotron Radiation Lightsource (SSRL). SSRL is operated by DOE and OBES. The SSRL SMB Program is supported through DOE, OBER, and by the NIH, the National Center for Research Resources (NCRR).

REFERENCES

(1) (a) Shook, R. L.; Borovik, A. S. *Inorg. Chem.* **2010**, *49*, 3646−3660. (b) Shook, R. L.; Borovik, A. S. *Chem. Commun.* **2008**, 6095−6107. (c) Borovik, A. S. *Acc. Chem. Res.* **2005**, *38*, 54−61. (d) Sigman, J. A.; Kim, H. K.; Zhao, X.; Carey, J. R.; Lu, Y. *Proc. Natl. Acad. Sci. U.S.A.* **2003**, *100*, 3629−3634. (e) Lu, Y. *Inorg. Chem.* **2006**, *45*, 9930−9940. (f) Lu, Y.; Yeung, N.; Sieracki, N.; Marshall, N. M. *Nature* **2009**, *460*, 855. (g) Lu, Y.; Berry, S. M.; Pfister, T. D. *Chem. Rev.* **2001**, *101*, 3047−f3080. (h) Natale, D.; Mareque-Rivas, J. C. *Chem. Commun.* **2008**, 425−437.

(2) (a) Schurmann, K.; Anton, M.; Ivanov, I.; Richter, C.; Kuhn, H.; Walther, M. *J. Biol. Chem.* **2011**, *286*, 23920−23927. (b) Saam, J.; Ivanov, I.; Walther, M.; Hozhütter, H. G.; Kuhn, H. *Proc. Natl. Acad. Sci. U.S.A.* **2007**, *104*, 13319−13324. (c) Schenk, G.; Neidig, M. L.; Zhou, J.; Holman, T. R.; Solomon, E. I. *Biochemistry* **2003**, *42*, 7294−7302.

(3) Umena, Y.; Kawakami, K.; Shen, J.; Kamiya, N. *Nature* **2011**, *473*, 55−61.

(4) (a) Barry, B. A.; Chen, J.; Keough, J.; Jenson, D.; Offenbacher, A.; Pagba, C. *J. Phys. Chem. Lett.* **2012**, *3*, 543−554. (b) Saito, K.; Shen, J.-

R.; Ishida, T.; Ishikita, H. *Biochemistry* **2011**, *50*, 9836−9844. (c) Haumann, M.; Junge, W. *Biochim. Phys. Acta* **1999**, *1411*, 121−133. (d) Saito, K.; Shen, J.-R.; Ishida, T.; Ishikita, H. *Biochemistry* **2011**, *50*, 9836−9844. (e) Hwang, H. J.; Dilbeck, P.; Debus, R. J.; Burnap, R. L. *Biochemistry* **2007**, *46*, 11987−11997. (f) Meyer, T. J.; Huynh, M. H. V.; Thorp, H. H. *Angew. Chem., Int. Ed.* **2007**, *46*, 5284−5304. (g) Polander, B. C.; Barry, B. A. *Proc. Natl. Acad. Sci. U.S.A.* **2012**, *109*, 6112−6117.

(5) (a) Ghanotakis, D. F.; Babcock, G. T.; Yocum, C. F. *FEBS Lett.* **1984**, *167*, 120−130. (b) Boussac, A.; Rutherford, A. W. *Biochemistry* **1988**, *27*, 3476−3483. (c) Ananyev, G. A.; Zaltsman, L.; Vasko, C.; Dismukes, G. C. *Biochim. Biophys. Acta* **2001**, *1503*, 52−68. (d) Yocum, C. F. *Coord. Chem. Rev.* **2008**, *252*, 296−305. (e) Miqyass, M.; van Gorkom, H. J.; Yocum, C. F. *Photosynth. Res.* **2007**, *92*, 275−287. (f) Miqyass, M.; Yocum, C. F.; van Gorkom, H. J. Calcium Requirements for S-State Transitions. In *Photosynthesis. Energy from the Sun*; Allan, J. F., Gantt, E., Golbeck, J. H., Osmond, B., Eds.; Springer: Amsterdam, The Netherlands, 2008; pp 459−462. (g) Pecoraro, V. L.; Baldwin, M. J.; Caudle, M. T.; Hsieh, W.-Y.; Law, N. A. *Pure Appl. Chem.* **1998**, *70*, 925−929. (h) Cady, C. W.; Crabtree, R. H.; Brudvig, G. W. *Coord. Chem. Rev.* **2008**, *252*, 444−455. (i) Brudvig, G. W. *Philos. Trans. R. Soc., B* **2008**, *8*, 1211−1219. (j) Mullins, C. S.; Pecoraro, V. L. *Coord. Chem. Rev.* **2008**, *47*, 1849−1861. (k) Betley, T. A.; Wu, Q.; VanVoorhis, T.; Nocera, D. G. *Inorg. Chem.* **2008**, *47*, 1894−1861.

(6) (a) Wiechen, M.; Zaharieva, I.; Dau, H.; Kurz, P. *Chem. Sci.* **2012**, DOI: 10.1039/C2SC20226C. (b) Kanan, M. W.; Nocera, D. G. *Science* **2008**, *321*, 1072−1075. (c) Reece, S. Y.; Hamel, J. A.; Sung, K.; Jarvi, T. D.; Esswein, A. J.; Pijpers, J. J. H.; Nocera, D. G. *Science* **2011**, *334*, 645−648.

(7) (a) Kotzabasaki, V.; Siczek, M.; Lis, T.; Milios, C. J. *Inorg. Chem. Commun.* **2011**, *14*, 213−216. (b) Nayak, S.; Nayek, H. P.; Dehnen, S.; Powell, A. K.; Reedijk, J. *Dalton. Trans.* **2011**, *40*, 2699−2702. (c) Hewitt, I. J.; Tank, J.-K.; Madu, N. T.; Clérac, R.; Buth, G.; Anson, C. E.; Powell, A. K. *Chem. Commun.* **2006**, 2650−2652. (d) Mishra, A.; Wernsorfer, W.; Abboud, K. A.; Christou, G. *Chem. Commun.* **2005**, 54−56.

(8) Kanady, J. S.; Tsui, E. Y.; Day, W. M.; Agapie, T. *Science* **2011**, *333*, 733−736.

(9) Park, Y. J.; Ziller, J. W.; Borovik, A. S. *J. Am. Chem. Soc.* **2011**, *133*, 9258−9261.

(10) Pfaff, F. F.; Kundu, S.; Risch, M.; Pandian, S.; Heims, F.; Pryjomska-Ray, I.; Haack, P.; Metzinger, R.; Bill, E.; Dau, H.; Comba, P.; Ray, K. *Angew. Chem., Int. Ed.* **2011**, *50*, 1711−1715.

(11) (a) Margulieux, G. W.; Weidermann, N.; Lacy, D. C.; Moore, C. E.; Rheingold, A. L.; Figueroa, J. S. *J. Am. Chem. Soc.* **2010**, *132*, 5033−5035. (b) Connelly, N. G.; Geiger, W. E. *Chem. Rev.* **1996**, *96*, 877−910. (c) Panda, T. K.; Hrib, C. G.; Jones, P. G.; Jenter, J.; Roesky, P. W.; Tamm, M. *Eur. J. Inorg. Chem.* **2008**, 4270−4279. (d) Dauban, P.; Saniere, L.; Tarrade, A.; Dodd, R. H. *J. Am. Chem. Soc.* **2001**, *123*, 7707−7708.

(12) See Supporting Information for experimental details.

(13) (a) Walsh, P. J. *Acc. Chem. Res.* **2003**, *36*, 739−749. (b) Walsh, P. J.; Lurain, A. E.; Balsells, J. *Chem. Rev.* **2003**, *103*, 3297−3344. (c) Pritchett, S.; Woodmansee, D. H.; Gantzel, P.; Walsh, P. J. *J. Am. Chem. Soc.* **1998**, *120*, 6423−6424. (d) Nanthakumar, A.; Miura, J.; Diltz, S.; Lee, C.-K.; Aguirre, G.; Ortega, F.; Ziller, J. W.; Walsh, P. J. *Inorg. Chem.* **1999**, *38*, 3010−3013.

(14) (a) Schwarz, A. D.; Chu, Z.; Mountford, P. *Organometallics* **2010**, *29*, 1246−1260. (b) Schwarz, A. D.; Herbert, K. R.; Paniagua, C.; Mountford, P. *Organometallics* **2010**, *29*, 4171−4188.

(15) (a) Ray, M.; Hammes, B. S.; Yap, G. P. A.; Rheingold, A. L.; Borovik, A. S. *Inorg. Chem.* **1998**, *37*, 1527−1532. (b) Lucas, R. L.; Zart, M. K.; Murkerjee, J.; Sorrell, T. N.; Powell, D. R.; Borovik, A. S. *J. Am. Chem. Soc.* **2006**, *128*, 15476−15489. (c) Hammes, B. S.; Young, G. V., Jr.; Borovik, A. S. *Angew. Chem., Int. Ed.* **1999**, *38*, 666−669. (d) Larsen, L. P.; Parolin, T. J.; Powell, D. R.; Hendrich, M. P.; Borovik, A. S. *Angew. Chem., Int. Ed.* **2003**, *42*, 85−89.

(16) (a) Ciampolini, M. Spectra of 3d Five-Coordinate Complexes. In *Structure and Bonding*; Jorgenen, C. K., Neilands, J. B., Nyholm, R. S., Reinen, D., Williams, R. J. P., Eds.; Springer-Verlag: New York, 1969; Vol *6*, p 52−93. (b) Ciampolini, M.; Paoletti, P. *Inorg. Chem.* **1967**, *6*, 1261−1262. (c) Suh, M. P.; Lee, J.; Han, M. Y.; Yoon, T. S. *Inorg. Chem.* **1997**, *36*, 5651−5654. (d) Vaira, M. D.; Orioli, P. L. *Inorg. Chem.* **1967**, *6*, 955−957.

(17) (a) Banci, L.; Bencini, A.; Benelli, C.; Bohra, R.; Dance, J.-M.; Gatteschi, D.; Jain, V.; Mehrotra, R.; Tressaud, A.; Woolley, R.; Zanchini, C. Spectral-Structural Correlations in High-Spin Cobalt(II) Complexes. In *Structures Versus Special Properties, Structure and Bonding*; Springer Berlin: Heidelberg, Germany, 1982; Vol. *52*, pp 37−86. (b) Jenkins, D. M.; Bilio, A. J. D.; Allen, M. J.; Betley, T. A.; Peters, J. C. *J. Am, Chem. Soc.* **2002**, *124*, 15336−15350.

(18) We have spectrophotometrically monitored the formation of this Co^{II}−aquo species and found changes in the optical spectrum until 1 equiv of water was added to $[Co^{II}MST]^-$ and $Ca^{II}(OTf)_2$/15-crown-5; further addition of water caused no changes in the optical properties. Because we are only monitoring changes at the Co^{II} center, these findings suggest that only one water molecule affects the electronic transitions of the Co^{II} center (Figure S2), similar to what was observed for $[Co^{II}MST(OH_2)]^-$. However, these spectral data do not allow us to determine the exact structure of the complex in solution, in particular, the coordination spheres around the Ca^{II} center.

(19) This bond distance is comparable to the Co^{III}−O bond length of 1.894(2) Å reported for the monomeric $[Co^{III}H_3buea(OH)]^-$.[15c] However, this bond distance is longer than the average Co^{III}−O bond length found in a homobimetallic Co^{III} complex with a $Co^{III}_2(\mu\text{-}O)_2$ core.[15d]

(20) (a) The edge energies determined from the second derivative of the XANES spectra are 7716.40 eV for $[Co^{II}(\mu\text{-}OH_2)Ca^{II}OH_2]^+$ and 7717.82 eV for $[Co^{III}(\mu\text{-}OH)Ca^{II}]^+$. (b) Bonnitcha, P. D.; Hall, M. D.; Underwood, C. K.; Foran, G. J.; Zhang, M.; Beale, P. J.; Hambley, T. W. *J. Inorg. Biochem.* **2006**, *100*, 963−971. (c) Kanan, M. W.; Yano, J.; Surendranath, Y.; Dincâ, M.; Yachandra, V. K.; Nocera, D. G. *J. Am. Chem. Soc.* **2010**, *132*, 13692−13701.

(21) The kinetics of this reaction would allow for both the Co^{III}−OH and Co^{II}−OH_2 species to be present at the same time.

(22) (a) Dogutan, D. K.; McGuire, R., Jr.; Nocera, D. *J. Am. Chem. Soc.* **2011**, *133*, 9178−9180. (b) Dogutan, D. K.; Stoian, S. A.; McGuire, R., Jr.; Schwalbe, M.; Teets, T. S.; Nocera, D. G. *J. Am. Chem. Soc.* **2011**, *133*, 131−140. (c) Boyer, J. L.; Polyansky, D. E.; Szalda, D. J.; Zong, R.; Thummel, R. P.; Fujita, E. *Angew. Chem., Int. Ed.* **2011**, *50*, 12600−12604.

(23) Mareque-Rivas, J. C.; Prabaharan, R.; Rosales, R. T. M. *Chem. Commun.* **2004**, 76−77.

(24) Selected examples of the importance of redox-inactive metal ions on processes involving transition metal complexes: (a) Fukuzumi, S.; Ohkubo, K. *Chem.—Eur. J.* **2000**, *6*, 4532−4535. (b) Ohkubi, K.; Menon, S. C.; Orita, A.; Otera, J.; Fukuzumi, S. *J. Org. Chem.* **2003**, *68*, 4720−4726. (c) Darensbourg, M. Y.; Darensbourg, D. J.; Burns, D.; Drew, D. A. *J. Am. Chem. Soc.* **1976**, *98*, 3127−3136. (d) Gambarotta, Francesco, A.; Floriani, C.; Zanazzi, P. F. *J. Am. Chem. Soc.* **1982**, *104*, 5082−5092. (e) Lee, Y.; Mankad, N. P.; Peters, J. C. *Nat. Chem.* **2010**, *2*, 558−565. (f) Betley, T. A.; Peters, J. C. *J. Am. Chem. Soc.* **2003**, *125*, 10782−10783. (g) Ding, K.; Brennessel, W. W.; Holland, P. L. *J. Am. Chem. Soc.* **2009**, *131*, 10804−10805. (h) Ding, K.; Pierpont, A. W.; Brennessel, W. W.; Lukat-Rodgers, G.; Rodgers, K. R.; Cundari, T. R.; Bill, E.; Holland, P. L. *J. Am. Chem. Soc.* **2009**, *131*, 9471−9472. (i) Morimoto, Y.; Kotani, H.; Park, J.; Lee, Y.-M.; Nam, W.; Fukuzumi, S. *J. Am. Chem. Soc.* **2011**, *133*, 403−405. (j) Fukuzumi, S.; Morimoto, Y.; Kotani, H.; Naumov, P.; Lee, Y.-M.; Nam, W. *Nat. Chem* **2010**, *2*, 756−759. (k) Karlin, K. D. *Nat. Chem* **2010**, *2*, 711−712(d).

(25) (a) Goldsmith, C. R.; Cole, A. P.; Stack, T. D. P. *J. Am. Chem. Soc.* **2005**, *127*, 9904−9912. (b) Goldsmith, C. R.; Stack, T. D. P. *Inorg. Chem.* **2006**, *45*, 6048−6055. (c) Donoghue, P. J.; Tehranchi, J.; Cramer, C. J.; Sarangi, R.; Solomon, E. I.; Tolman, W. B. *J. Am. Chem. Soc.* **2011**, *133*, 17602−17605. (d) Ogo, S.; Wada, S.; Watanabe, Y.; Iwase, M.; Wada, A.; Harata, M.; Jitsukawa, K.; Masuda, H.; Einaga, H.

Angew. Chem., Int. Ed. **1998**, *37*, 2102−2104. (e) Ogo, S.; Yamahara, R.; Roach, M.; Suenobu, T.; Aki, M.; Ogura, T.; Kitagawa, T.; Masuda, H.; Fukuzumi, S.; Watanabe, Y. *Inorg. Chem.* **2002**, *41*, 5513−5520.
(26) Michel, C.; Baerends, E. J. *Inorg. Chem.* **2009**, *48*, 3628−3638.